



# Measuring the Thermal De-Broglie Wavelength in Laser-produced Plasma of different Samples of Writing Inks Elements Using LIBS Spectroscopy

Mohammed Abdullah Jasim<sup>1\*</sup>, Dr. Sami Abd Al-Hussein Hatif<sup>2</sup>, Dr. Alaa Hussein Ali<sup>3</sup>

## Abstract

In this paper, the technique of laser pulse breakdown spectroscopy (LIBS) under the influence of the pulse Nd:YAG laser of 1064nm wavelength and with a pulse time of 10ns was used on different samples of writing ink models. In this work, the de-Broglie wavelength was measured. After calculating the electron temperature and assuming the local thermal equilibrium conditions (LTE), and using a spectral detector model (View spectra 2100) within the spectral range (200nm-900nm), the results after performing the analysis showed differences in the D-Broglie thermal wavelength of the plasma. The formation and temperature of the electron, which can be applied in plasma spectroscopy processes in many sciences, including the field of forensic evidence, to detect forgery in documents and documents.

**Key Words:** De-Broglie Thermal Wavelength, LIBS, Electron Temperature, Writing Inks.

**DOI Number:** 10.14704/nq.2021.19.9.NQ21138

**NeuroQuantology 2021; 19(9):65-71**

65

## Introduction

The LIBS technique is one of the most promising technologies that analytical chemists have been able to develop, which works to determine the presence of elements in different material structures. As it depends on the excitation of the material to be analysed by this method on the use of laser energy that causes changes in the material (Williams, A., 2018).

In this technique, the laser is the main factor in the production of plasma, including the emission spectrum. The plasma is produced after dropping the laser pulse on the target material, sufficient to heat it and create a cloud of plasma on the surface of the sample and produce Seed Electrons by one or more process such as multi-photon ionization to produce an ionized plasma. The electrons allow more absorption of the energy of the laser pulse by

the process of reverse pulsar radiation, which in turn causes an increase in ionization. When these processes are renewed, they eventually lead to breakdown ionization due to the increase in the rate of ionization down to the plasma state, which prevents laser energy from the target material at a specific density called the critical density (Reinhard N., 2012; Vander Wal, 1999).

**Corresponding author:** Mohammed Abdullah Jasim

**Address:** <sup>1\*</sup>Department of Laser Physics, College of Sciences for Girls, University of Babylon, Iraq; <sup>2</sup>Department of Laser Physics, College of Sciences for Girls, University of Babylon, Iraq; <sup>3</sup>Ministry of Science & Technology, Iraq.

<sup>1\*</sup>E-mail: inklasermo@gmail.com

**Relevant conflicts of interest/financial disclosures:** The authors declare that the research was conducted in the absence of any commercial or financial relationships that could be construed as a potential conflict of interest.

**Received:** 07 July 2021 **Accepted:** 14 August 2021



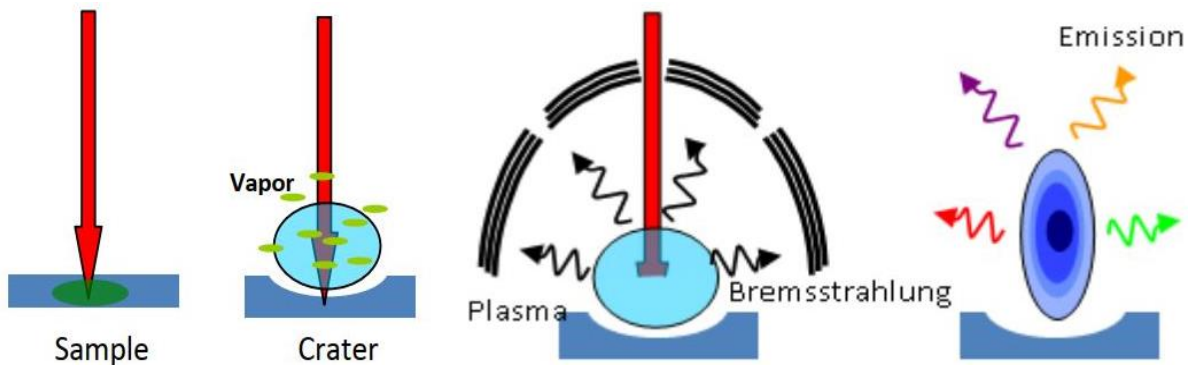


Figure 1. Basic LIBS Technology Processes (Peng, J., 2016).

When the plasma cools, these electrons will drop from higher energy levels to lower energy levels, which emit a plasma spectrum with different wavelengths for each element of the sample (Jelínková, H. ed., 2013).

### Experiment Setup and Procedure

The schematic diagram of the experimental setup of a laser induced breakdown spectroscopy is depicted in the Figure 2. A Q-switched Nd:YAG laser of 1064nm wavelength and with a pulse duration of 10ns and a repetition frequency of 1Hz with a laser energy of 140mJ was used on different samples of writing ink models and using a spectral detector model (View spectra 2100) within the spectral range (200nm-900nm).

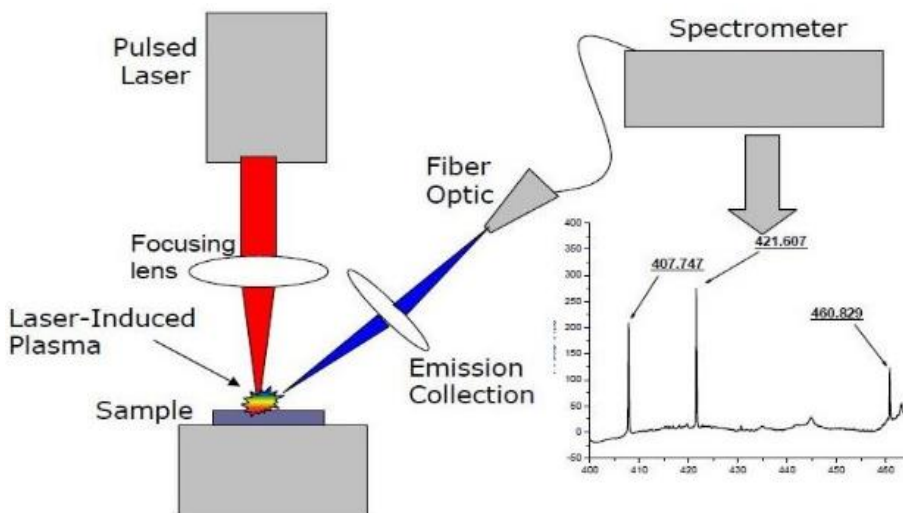


Figure 2. Schematic diagram of the experiment setup for laser induced breakdown spectroscopy

The detector that receives the emission and according to the wavelength of the samples, and then a special camera which is the charge-coupled device (CCD) records the resulting spectrum and when studying the type of emitted wavelengths and intensity, the type of elements in the sample can be diagnosed. The target and the amount of intensity must be fast responsive and for this a high-resolution optical spectrum analyser is used.

### Measuring the Electron Temperature

Assuming the conditions of local thermal equilibrium (LTE), the laws of equilibrium are fulfilled, including the Maxwell-Boltzmann law of velocity distribution and Saha's law (Huang, L. 2017). Therefore, the temperature of the plasma can be measured, which is a function that represents the temperatures of the particles inside the plasma and is measured in electron volts or Kelvin's. Here, the thermal kinetic energy of each molecule is measured



(Park, H., 2010). Using Boltzmann's equation, the electron temperature in the plasma is calculated as follows [Hussain, T., 2016]:

$$\ln\left(\frac{I \lambda}{A_{ki} g_k}\right) = -\frac{E_k}{K_B T_e} \quad (1)$$

Where  $E_k$  represents energy of the upper plane,  $I$  spectral intensity,  $A_{ki}$  transition probability,  $g_k$  statistical weight, and  $K_B$  Boltzmann constant.

### Measurement of the de-Broglie Thermal Wavelength of the Electron

The de-Broglie thermal wavelength of the electron in plasma, which is the approximate mean, can be measured using the following relationship (Cicconi, F., 2020):

$$\lambda_T = \left(\frac{2 \pi \hbar^2}{m K_B T_e}\right) \quad (2)$$

Where the reduced Planck constant  $m$  represents the mass of the particle,  $K_B$  is Boltzmann's constant;  $T$  represents the temperature of the electron.

This value gives an estimate of the quantitative nature of the plasma particles, and it is one of the most important quantities in the plasma generated by the laser pulse interacting with the target material.

### Results and Discussion

In this work, LIBS spectroscopy was used to analyse samples of writing inks, which is as shown in Table (1). Spectroscopy was performed for the components of these inks, measured the electron temperature of the generated plasma, and then measured the D-Broglie thermal wavelength of the electrons in it.

Table 1. Examined Samples

| sample | Brand         | olor  | Type | Source |
|--------|---------------|-------|------|--------|
| 1      | Sigma         | Blue  | Dry  | India  |
| 2      | Smart         | Blue  | Dry  | India  |
| 3      | Rebnok glaria | Blue  | Dry  | India  |
| 4      | Nataraj       | Blue  | Dry  | India  |
| 5      | Linc Axo      | Blue  | Dry  | India  |
| 6      | Montex Elite  | Black | Dry  | India  |
| 7      | Idea office   | Blue  | Dry  | China  |
| 8      | Montex LCD    | Blue  | Dry  | China  |

The emission spectra of these elements have been recorded and are shown in Figures (2), (3), (4), (5), (6), (7), (8), and (9) which describe the relationship between intensity versus wavelength.

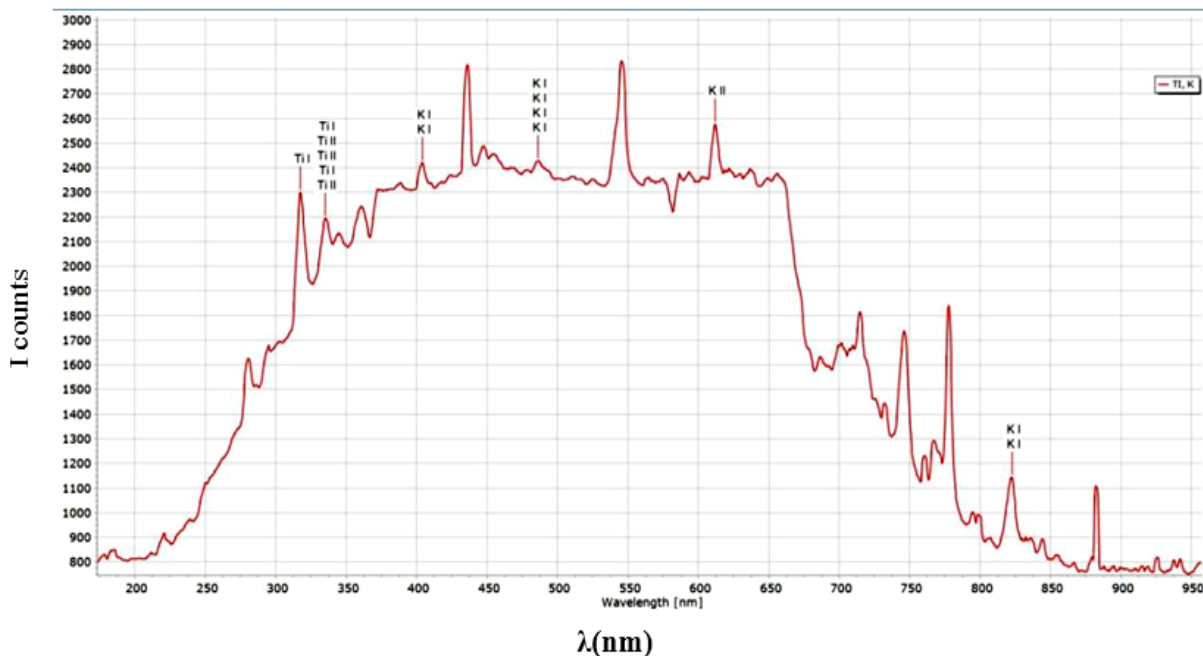


Figure 2. Emission spectrum of sample No. (1).



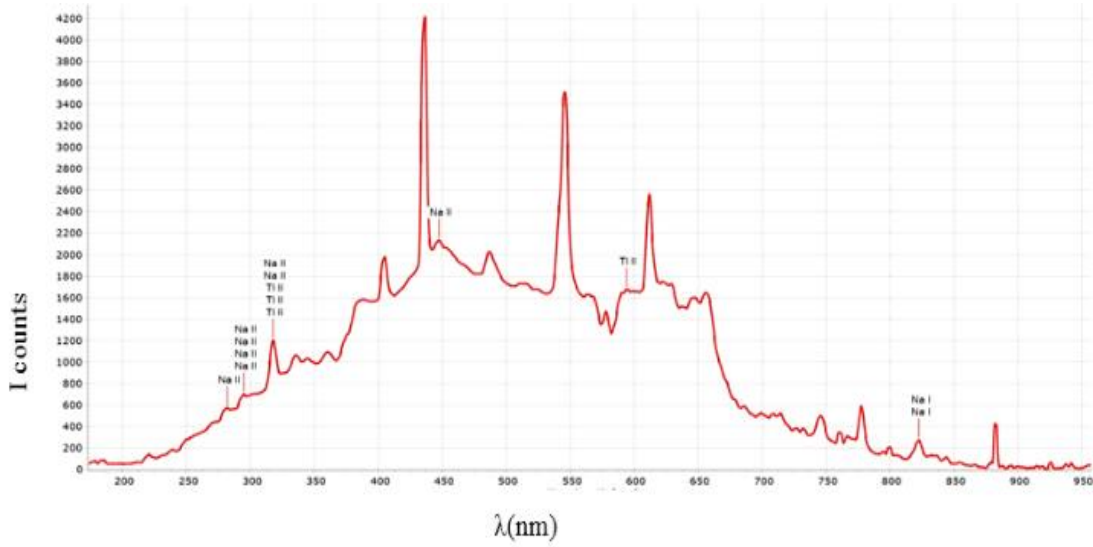


Figure 3. Emission spectrum of sample No. (2)

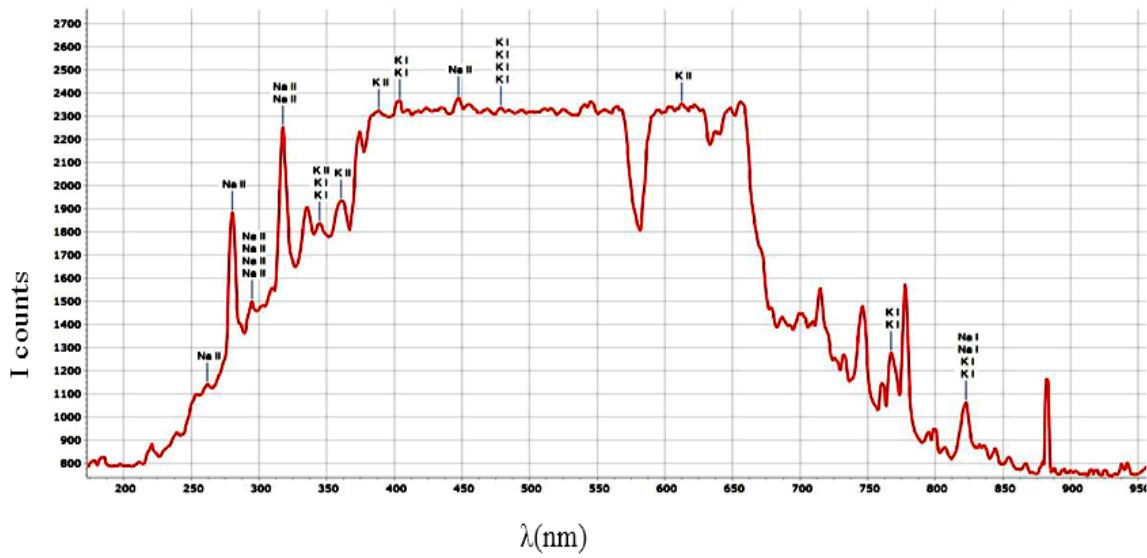


Figure 4. Emission spectrum of sample No. (3).

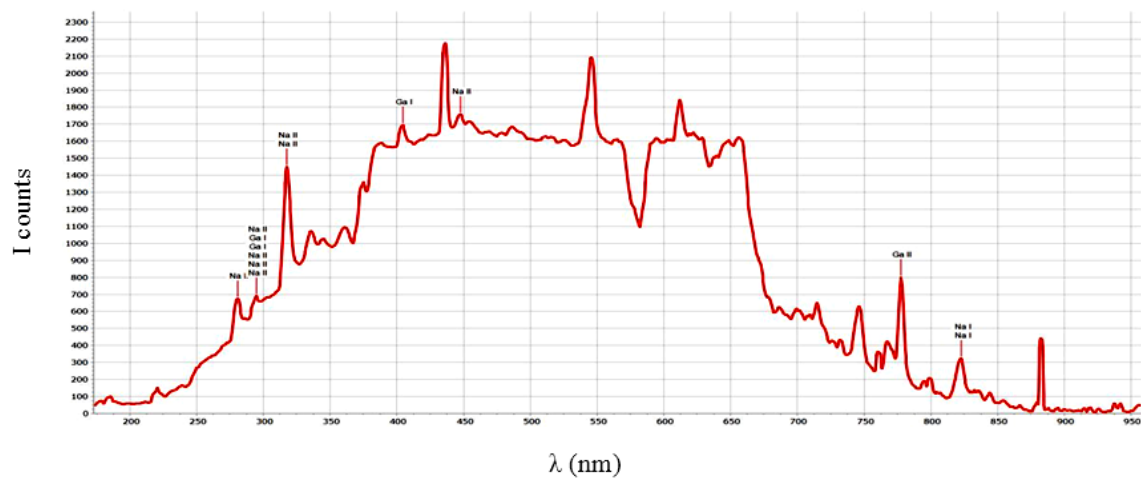


Figure 5. Emission spectrum of sample No. (4).



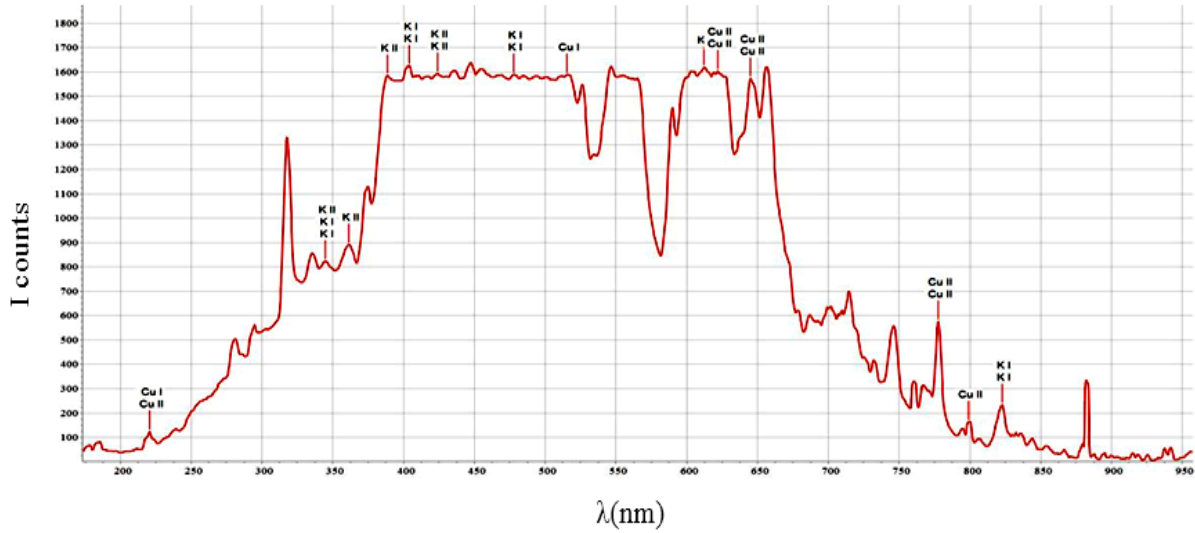


Figure 6. Emission spectrum of sample No. (5).

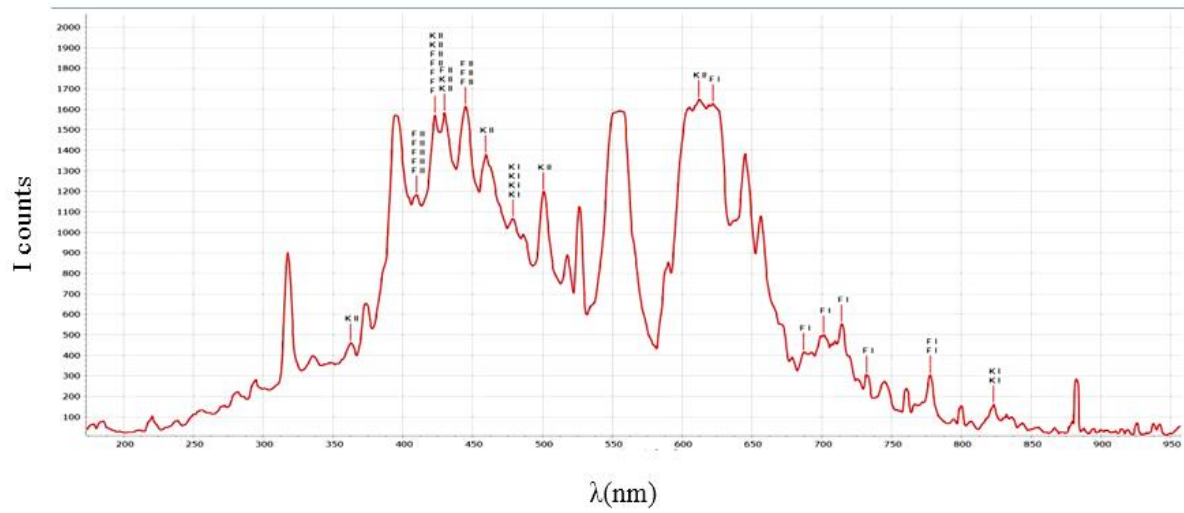


Figure 7. Emission spectrum of sample No. (6).

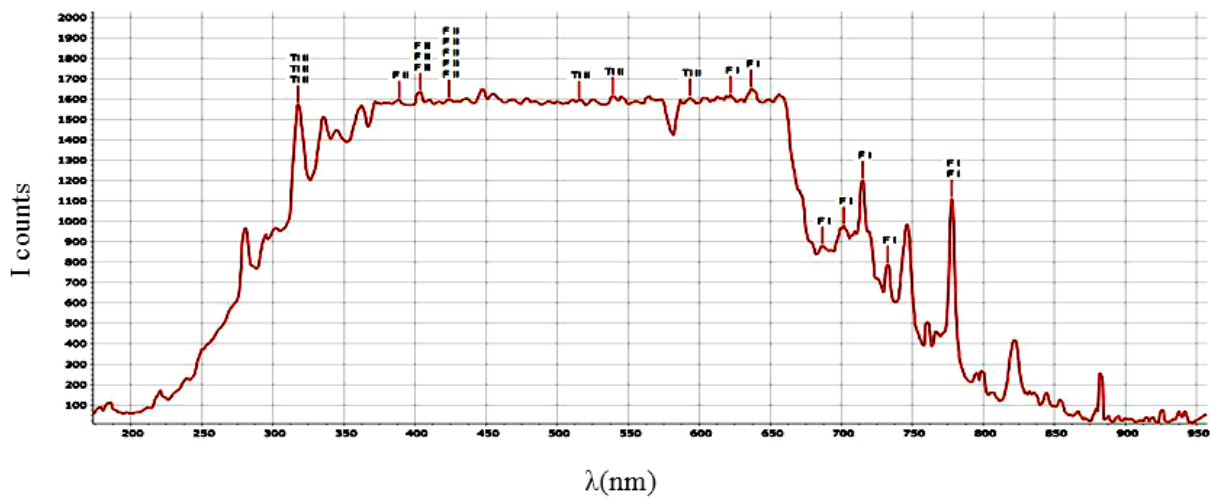


Figure 8. Emission spectrum of sample No. (7).



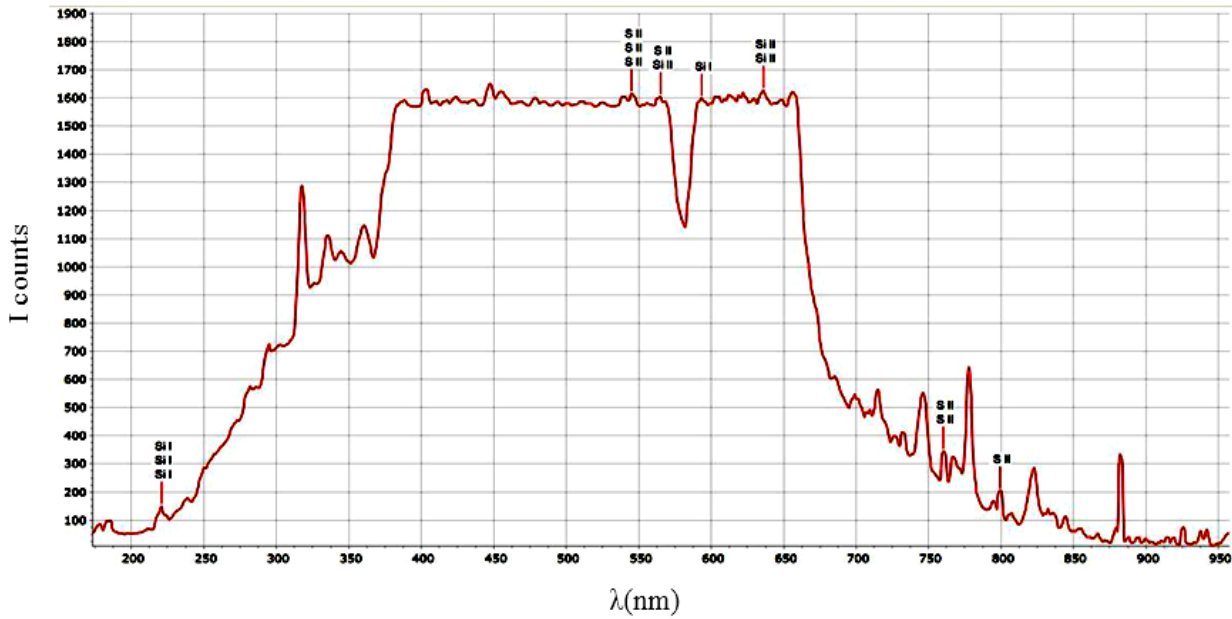


Figure 9. Emission spectrum of sample No. (8).

Table (2) shows the main emission lines for the sample elements whose data were recorded in this work, where the NIST spectroscopy database (NIST

At., 2019) was used which determines the type of spectral line, energies, transmission probability, and statistical weight.

Table 2. Data of the spectral emission lines for the examined elements

| No. | Ion   | λ LIBS (nm) | λ NIST (nm) | I (Counts) | A <sub>ki</sub> (s <sup>-1</sup> ) | g <sub>k</sub> Up. | E <sub>l</sub> (eV) | E <sub>u</sub> (eV) |
|-----|-------|-------------|-------------|------------|------------------------------------|--------------------|---------------------|---------------------|
| 1   | Ti I  | 317.51      | 317.55      | 2301.0     | 1.4E+08                            | 9                  | 2.134               | 6.034               |
| 1   | KI    | 486.30      | 486.34      | 2427.9     | 3.6E+08                            | 2                  | 1.017               | 4.165               |
| 2   | Ti I  | 317.57      | 317.55      | 1200.8     | 1.7E+08                            | 9                  | 2.134               | 6.034               |
| 2   | Na I  | 819.46      | 819.48      | 274.64     | 5.1E+07                            | 6                  | 2.104               | 3.616               |
| 3   | K I   | 825.06      | 825.01      | 1062.1     | 6.4E+07                            | 6                  | 2.669               | 4.172               |
| 3   | Na I  | 819.42      | 819.48      | 1062.1     | 5.1E+07                            | 6                  | 2.104               | 3.616               |
| 4   | Na I  | 819.47      | 819.48      | 323.48     | 5.1E+07                            | 6                  | 2.104               | 3.616               |
| 4   | GaII  | 779.20      | 779.22      | 789.48     | 7.1E+07                            | 9                  | 13.355              | 14.940              |
| 5   | Cu I  | 515.31      | 515.32      | 1588.6     | 6.0E+07                            | 4                  | 3.785               | 6.191               |
| 5   | KI    | 825.02      | 825.01      | 233.35     | 6.4E+04                            | 6                  | 2.669               | 4.172               |
| 6   | K I   | 825.01      | 825.01      | 160.1      | 6.4E+04                            | 6                  | 2.669               | 4.172               |
| 6   | F I   | 712.75      | 712.78      | 552.66     | 5.0E+08                            | 2                  | 13.025              | 14.764              |
| 7   | Ti II | 539.12      | 539.12      | 1613.5     | 1.2E+08                            | 8                  | 5.567               | 7.866               |
| 7   | F I   | 780.00      | 780.02      | 1110.3     | 2.5E+07                            | 4                  | 5.280               | 6.960               |
| 8   | S II  | 545.90      | 545.91      | 1613.9     | 5.9E+08                            | 3                  | 8.045               | 10.125              |
| 8   | Si II | 637.10      | 637.13      | 1627.2     | 6.8E+08                            | 2                  | 8.121               | 10.060              |

The electron temperature (Te) and the D-Broglie thermal wavelength were measured using equations (1) and (2). As shown in Table (3).



**Table 3.** The values of the electron temperature and the thermal de-Broglie wavelength for some ink elements recorded from the examined samples

| Sample No. | Element | $T_e$ (K) | $\lambda_T$ (cm) |
|------------|---------|-----------|------------------|
| 1          | Ti I    | 9395.91   | 7.14E-10         |
| 1          | KI      | 7536.9    | 7.97E-10         |
| 2          | Ti I    | 8439.56   | 7.53E-10         |
| 2          | Na I    | 5816.18   | 9.07E-10         |
| 3          | K I     | 7959.54   | 7.37E-10         |
| 3          | Na I    | 7158.0    | 8.18E-10         |
| 4          | Na I    | 5951.3    | 5.05E-10         |
| 4          | Ga II   | 18777.5   | 8.97E-10         |
| 5          | Cu I    | 12461.4   | 6.02E-10         |
| 5          | K I     | 7012.1    | 8.26E-10         |
| 6          | K I     | 4536.7    | 1.03E-09         |
| 6          | F I     | 2185.9    | 4.68E-10         |
| 7          | Ti II   | 13028.9   | 6.06E-10         |
| 7          | F I     | 17008.0   | 5.31E-10         |
| 8          | S II    | 15449.6   | 5.57E-10         |
| 8          | Si II   | 9630.2    | 7.05E-10         |

## Conclusions

The results were clarified after examining different ink samples in this work, which were of different origins and types, using LIBS plasma breakdown spectroscopy, analysing them and recording the results, we conclude the following:

1. The clarity of the rate of differences in the calculated values of the electron temperature and the de-Broglie thermal wavelength can be used in the study of the performance of the plasma formed by the laser pulse.
2. The results of the recorded analysis and the calculated values of the samples have shown that LIBS is a good method in detecting and studying the elements of writing inks that can be used in the field of forensic science to detect forgery in documents due to the difference in their values.
3. LIBS spectroscopy is reliable at identifying the elements in the components of writing inks without affecting or damaging the target sample by a laser pulse. The emission spectra of the elements of these samples were recorded and the relationship between intensity and wavelength was found.
4. The source of irritation and excitement of the samples, which is the laser, is an important tool to obtain a plasma, which works with the technique of (Q-Switching) passive because of the results consistency with the international experimental results.

## Thanks

I have the honour to dedicate the most sincere feelings of love and respect to everyone who helped me, my distinguished professors, Head of the Physics Department, College of Science for Woman / University of Babylon, I reiterate my heartfelt and eternal thanks. And to your Journal staff for giving me the opportunity to publish in it.

## References

- Cicconi F, Lazic V, Palucci A, Almeida Assis AC, Saverio Romolo F. Forensic analysis of commercial inks by laser-induced breakdown spectroscopy (LIBS). *Sensors* 2020; 20(13): 3744.
- Huang L, Chen T, He X, Yang H, Wang C, Liu M, Yao M. Determination of heavy metal chromium in pork by laser-induced breakdown spectroscopy. *Applied Optics* 2017; 56(1): 24-28.
- Hussain T, Gondal MA, Shamraiz M. Determination of plasma temperature and electron density of iron in iron slag samples using laser induced breakdown spectroscopy. *In IOP Conference Series: Materials Science and Engineering* 2016; 146(1).
- Jelínková, H. *Lasers for medical applications: diagnostics, therapy and surgery*. Elsevier 2013.
- NIST At. *National Institute of Standards and Technology*. Gaithersburg, MD 2019. <http://physics.nist.gov/asd> (2019).
- Park H, You SJ, Choe W. Correlation between excitation temperature and electron temperature with two groups of electron energy distributions. *Physics of Plasmas* 2010; 17(10).
- Peng J, Kong W, Liu F, Song K, Ye L, He Y. Fast determination of heavy metal in tobacco leaves by laser-induced breakdown spectroscopy. *In ASABE Annual International Meeting 1. American Society of Agricultural and Biological Engineers* 2016.
- Noll R. *Laser-induced breakdown spectroscopy*. In *Laser-Induced Breakdown Spectroscopy*, Springer, Berlin, Heidelberg 2012: 7-15. <http://doi.org/10.1007/978-3-642-20668-9>
- Vander Wal RL, Ticich TM, West JR, Householder PA. Trace metal detection by laser-induced breakdown spectroscopy. *Applied Spectroscopy* 1999; 53(10): 1226-1236.
- Williams A, Phongikaroon S. Laser-Induced Breakdown Spectroscopy (LIBS) Measurement of Uranium in Molten Salt. *Applied Spectroscopy* 2018; 72(7): 1029-1039.
- Lu YB, Cai ZY, He GG, Zhao JY, Chen YT, Zheng SM, Kang XW. Research progress of microRNA in spinal cord injury. *NeuroQuantology* 2019; 17(7): 23-28.

